Spontaneous-Curvature Theory of Clathrin-Coated Membranes

Robert J. Mashl* and Robijn F. Bruinsma#
*Department of Chemistry and Biochemistry, and #Department of Physics and Astronomy, University of California at Los Angeles, Los Angeles, California 90095 USA

ABSTRACT Clathrin-coated membranes are precursors to coated vesicles in the receptor-mediated endocytic pathway. In this paper we present a physical model for the first steps of the transformation of a clathrin-coated membrane into a coated vesicle. The theory is based on in vitro cytoplasmic acidification experiments of Heuser (*J. Cell Biol.* 108:401–411) that suggest the transformation proceeds by changes in the chemical environment of the clathrin lattice, wherein the chemical environment determines the amount of intrinsic, or spontaneous, curvature of the network. We show that a necessary step of the transformation, formation of free pentagons in the clathin network, can proceed via dislocation unbinding, driven by changes in the spontaneous curvature. Dislocation unbinding is shown to favor formation of coated vesicles that are quite small compared to those predicted by the current continuum theories, which do not include the topology of the clathrin lattice.

NOMENCLATURE

F; F_b, F_L, F_s, F_t, F_{var}, F_{sc}	free energy; bending, line, stretching total, variational, spontaneous-curvature free energies
κ, κ_G, τ	bending, splay, line energies
E_B	clathrin bond energy
R, R_b, r_0	radius, buckling radius, lattice constant
$c_0^{(*)}$	spontaneous curvature (critical)
H, K	total, Gaussian curvatures
Γ	control parameter
$\mathbf{u}$, f	in-plane, out-of-plane deformation functions
u_{ij}	strain tensor
$\mathbf{b}$, s	Burger's vector, disclinicity
K_0	2-D Young's elastic modulus
λ, μ	2-D Lamé elastic moduli
θ_5', θ_7'	variational angles
k_B	Boltzmann's constant
T	absolute temperature

INTRODUCTION

Endocytosis is a fundamental biological process that serves as a primary mechanism for transport of extracellular material into cells (for a general reference, see e.g., Alberts et al., 1994). During endocytosis a region of cell membrane deepens into the cytoplasm to produce a "bud" that eventually detaches, or vesiculates, to produce an internal vesicle. Eukaryotic cells in particular have portions of the cytosolic side of their plasma membranes lined with a proteinaceous layer. Electron microscopy studies first revealed that these regions, or "coated" pits, are slightly indented, specialized regions on the cell membrane and suggested they were precursors of intracellular coated vesicles (Roth and Porter, 1964). Coated pits mediate the selective uptake of a variety of macromolecules through receptor-mediated endocytosis (for reviews, see Goldstein et al., 1979; Pastan and Willingham, 1981; Pearse, 1980). Among these macromolecules are, for example, low-density lipoproteins (Anderson, 1976), which provide the raw materials for the manufacture of cholesterol, a necessary component in regulating the fluidity of plasma membranes.

The nature of the coats in coated membranes and coated vesicles has been the subject of many studies. Electron microscopy studies have revealed that the basic structure of these coated vesicles is that of a lipid vesicle surrounded by a closed network of hexagonal and pentagonal facets (Kanaseki and Kadota, 1969). Pearse (1975) had analyzed the coats of these vesicles and found they consist of a single protein subunit (of 180,000 Da) that she named clathrin. Heptagons, in addition to the usual hexagons and pentagons, were shown by electron microscopy to exist in the polygonal networks of clathrin-coated pits (Fig. 1; Heuser, 1980). Rotary-shadowing visualization techniques have shown the clathrin molecule to be a triskelion with three kinked arms extending outward from a central vertex (Ungewickell and Branton, 1981). Fig. 2 shows electron micrographs of a clathrin molecule and a schematic of its three major functional parts: a proximal section closest to the vertex, a distal section, and a terminal domain (Kirchhausen and Harrison, 1981, 1984; Ungewickell and Branton, 1981). There is one clathrin molecule for each vertex in the clathrin coats (Crowther et al., 1976; Kirchhausen and Harrison, 1981). Each polyhedral edge in the clathrin network consists of a bundle of four arms: one proximal segment from each of two neighboring triskelions and one distal segment from each of two nearby triskelions (Crowther and Pearse, 1981). In Fig. 3 we show a version of Fig. 1, showing only the overlapping of proximal sections, for clarity. The lattice constant of this clathrin network is ~17 nm. In coated vesicles the terminal domains are directed into the interior, as evidenced by freeze-etching studies (Heuser and Kirch-

Received for publication 18 June 1997 and in final form 12 March 1998.
Address reprint requests to Dr. Robert J. Mashl, T-CNLS, MS B258, Los Alamos National Laboratory, Los Alamos, NM 87545. Tel.: 505-665-0612; Fax: 505-665-2659; E-mail: mashl@lanl.gov.

0006-3495/98/06/2862/14 $2.00

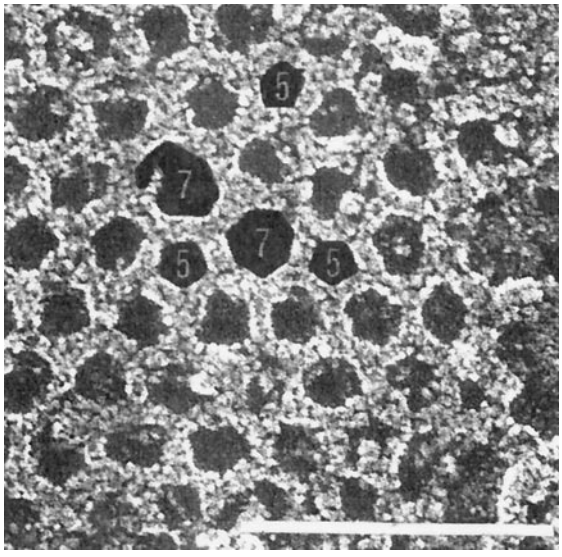

FIGURE 1 A region of clathrin network, showing dislocations and an isolated pentagon. The arrow indicates an incomplete polygon. Bar, 0.1 μm. Reproduced from Heuser (1980) by permission of The Rockefeller University Press.

hausen, 1985) and by three-dimensional image reconstructions from electron micrographs of clathrin cages in vitreous ice (Vigers et al., 1986).

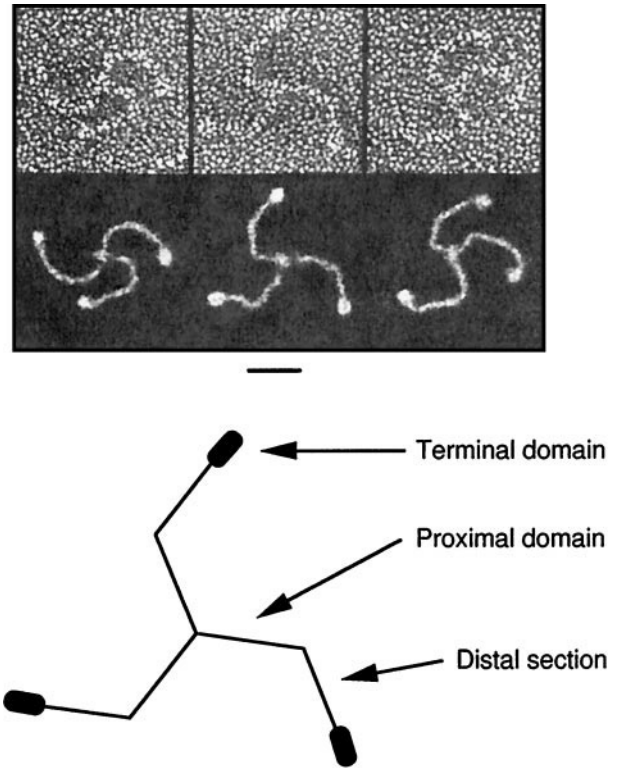

FIGURE 2 (*Top*) Digitized electron micrographs of individual clathrin molecules and their reconstructed images. Bar, 25 nm. Reproduced from Steven (1983). (*Bottom*) Idealized view of the clathrin molecule and its functional parts.

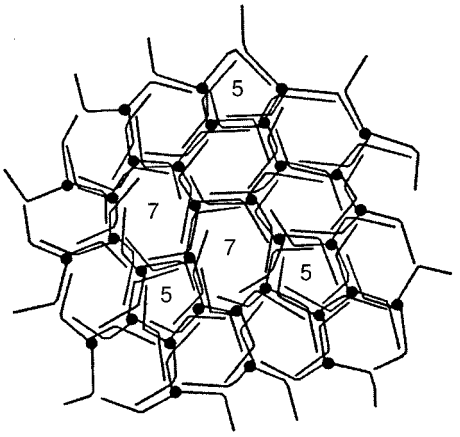

FIGURE 3 Sketch of the clathrin network in Fig. 1, showing the most probable packing (Crowther and Pearse, 1981; Keen, 1985) of the clathrin molecules, modified from Jin and Nossal (1993). The terminal domains are bent beneath the lattice and are omitted. Polygonal edges consist of the interactions among two distal sections and two proximal sections.

The aim of this paper is to develop a physical description for clathrin-coated membranes in the spirit of the thermodynamic descriptions already developed for clathrin-free, artificial phospholipid membranes. Of particular interest is the question of size selection: What are the factors that determine the size of a clathrin-coated vesicle? Experiments on in vivo coated vesicles reveal a distribution of sizes, depending on the tissue type of the cell (Steven et al., 1983, and references therein) and on the particular membranes within the cell (Bomsel et al., 1986; Kedersha et al., 1986). A broad distribution of coated-vesicle sizes is found, ranging from ~70 nm in diameter (Bomsel et al., 1986) to 350 nm (Perry and Gilbert, 1979). These typical sizes are quite small, however, compared to unsonicated, pure phospholipid vesicles whose sizes are in the range of 10–50 μm. The formation of pure phospholipid vesicles can be understood rather well by using the continuum description of fluid membranes (Lipowsky, 1993). One of the aims of this paper is to construct a continuum theory of membranes that includes the effects of the clathrin coating and can address the size selection question.

Kinetics and energetics of clathrin coats

A physical description of the budding of coated pits and their vesiculation into coated vesicles first requires answers to two important questions whose answers are not fully known. The first question is kinetic: What is the lattice transformation mechanism that converts a patch of clathrin network into a clathrin-coated vesicle? Micrographs of freeze-fractured, real cells (Heuser, 1980) and reassembled, in vitro clathrin lattices (Moore et al., 1989) have shown that (flat) extended hexagonal arrays of clathrin can exist on the inside surfaces of the plasma membrane. From topological considerations it is clear that a flat, regular hexagonal lattice cannot be deformed into a spherical cage without

introducing lattice defects. These defects or disclinations are centers of nonhexagonal symmetry. Indeed, a mathematical theorem of Euler (Lord and Wilson, 1984) for simple, closed polyhedra states that the total number of faces and vertices exceeds the number of edges by precisely 2. Clathrin networks normally contain only five-, six-, and seven-sided facets. A disclination with a local fivefold symmetry imparts a conelike structure to the coat, whereas a disclination with a sevenfold local symmetry imparts a saddle-like structure. Euler's theorem implies that precisely 12 pentagons, plus a variable number of hexagons, are required to form a closed cage. Thus, for a flat, hexagonal clathrin network to gain sufficient curvature to form a closed cage, the connectivity of the network due to the associations between the arms of the clathrin molecules (see Fig. 3) must change. We conclude that if a patch of the clathrin-covered membrane is to lead to a clathrin-coated vesicle, there must exist a mechanism for the formation of pentagons in the clathrin lattice.

Mechanisms that have been proposed to describe the formation of pentagons fall into two classes. In the edge-acquisition hypothesis, pentagons are assumed to form at the edge of a patch of clathrin network. In one scenario pentagons diffuse into the hexagonal array via the production of a series of dislocations (i.e., pentagon-heptagon pairs) (Pearse and Bretscher, 1981). Indeed, not only have pentagons with neighboring heptagons been observed in patches of network, but also the edges of the patches of network have appeared to contain incomplete polygons, suggesting that lattice growth involves assembly at the edge (Heuser, 1980; Larkin et al., 1986). Shraiman (1997) has recently proposed a thermal ratchet-like growth scenario for coated pits in which the curvature fluctuations of the plasma membrane accommodate the incorporation of edge pentagons.

The second class of proposed mechanisms for the production of pentagons involves interior-acquisition hypotheses. One hypothesis asserts that dislocations are first produced inside the hexagonal array by transforming two neighboring hexagons into a neighboring pentagon-heptagon pair, after which the heptagons move toward the edge of the hexagonal lattice (Pearse and Bretscher, 1981). Frozen-in dislocations in the clathrin network could similarly be a source of free pentagons. A second hypothesis is a topological mechanism in which pentagons are formed through the addition of clathrin dimers to the interior of a patch of hexagonal network (Jin and Nossal, 1993). This addition, in conjunction with internal rearrangements of the clathrin arms (and, hence, polygonal edges), again leads to the creation of pentagon-heptagon pairs. The addition of more dimers results in a network containing a group of pentagons surrounded by a ring of heptagons, a structure whose appearance suggests incipient vesiculation. These kinetic scenarios thus all require topological changes in the clathrin network, as imposed by Euler's theorem.

The second important question regarding the budding and vesiculation of clathrin-coated membranes is energetic: What is the energetic mechanism driving these topological transformations? Dissociation of clathrin coats are known to require hydrolysis of about three to four ATP molecules per clathrin molecule released (Braell et al., 1984). The energy released by the hydrolysis provides approximately $E_B = 20–30k_BT$ ($\sim$12–18 kcal/mol) of free energy to break the bonding that occurs among the four clathrin arms in a polygonal edge. We infer from these values that 1) diffusive motion of pentagons or heptagons induced by thermal fluctuations is rather unlikely and 2) the energetic mechanism responsible for the production of pentagons must be sufficiently powerful to be able to rupture individual clathrin links. An interesting paradox concerning the energy barrier that must be overcome for this process to start has been pointed out by Kirchhausen (1993; Harrison and Kirchhausen, 1983). If we assume the conventional scenario that coated vesicles originate from coated pits (Roth and Porter, 1964; Pearse and Crowther, 1987), then the conversion of a hexagon to a pentagon inside an otherwise hexagonal clathrin network requires the excision of a 60° wedge from the network. The free energy cost for this process would be on the order of the free energy cost of rupturing a single clathrin bond E_B times the number of bonds broken (i.e., twice the radius of the patch R divided by the network lattice constant r_0). Because $E_B = 20–30k_BT$, the overall free energy cost could be many hundreds of k_BT, seemingly forbidding the conventional scenario. Resolving this paradox is one of the aims of this paper.

A series of experiments by Heuser has provided insight into the energetics of the transformation process. Under normal physiological conditions, clathrin-coated membranes contain large regions of flat clathrin network (Heuser, 1980). The in vivo acidification of the extracellular medium and the in vitro acidification of exposed clathrin lattices both lead to the formation of so-called microcages of clathrin that nucleate near or at the edges of a region of clathrin network (see Fig. 4) (Heuser, 1989). These microcages, almost perfectly spherical, with a radius of $\sim$25–30 nm, are small compared to endocytosed coated vesicles and are devoid of any cell membrane. Heuser's observations indicate that the driving force for the formation of coated vesicles is the chemical asymmetry of the clathrin network. By this we mean that the clathrin network does not have in-plane mirror symmetry. The clathrin network is of course asymmetrical because it covers only one side of the membrane bilayer, but the asymmetry at the molecular level is already evident from Fig. 2: individual clathrin molecules adsorbed on a flat substrate have a handedness. As a consequence, clathrin molecules forming a network covering a membrane will tend to induce a finite mean curvature to the membrane. Heuser's experiments indicate that this mean curvature is adjustable by the pH level and by other environmental conditions and, as can be deduced from the formation of the microcages, that a clathrin network can have such a pH-controlled curvature, even in the absence of a membrane bilayer.

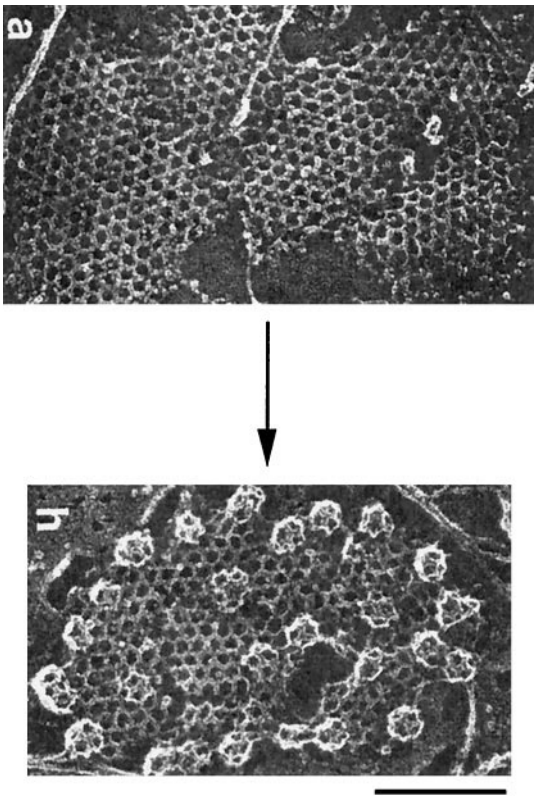

FIGURE 4 A clathrin network initially at neutral pH is acidified to pH 5.5–6.0, resulting in the formation of "microcages," which are devoid of cell membrane and inhibit endocytosis. Bar, 0.2 μm. Reproduced from Heuser (1989) by permission of The Rockefeller University Press.

How can the spontaneous curvature due to chemical asymmetry produce the required topological changes in the network? Consider, for example, a flat, hexagonal patch of clathrin-coated membrane with no defects. If the spontaneous curvature of the composite increases, starting from zero, by lowering the extracellular pH or by some other means, the flat patch will at first deform into a curved bowl without any changes in the network topology. Because bending an initially flat, regular network is impossible without distorting the lattice bonds, the arms of at least some of the clathrin molecules in the curved bowl must become deformed, thereby introducing elastic stress into the clathrin network. As the spontaneous curvature is increased further, the build-up of stress in the network must lead to rupture somewhere. As we mentioned earlier, this rupture must lead to the production of pentagons, either at the edge (an "edge acquisition" mechanism) or at one of the dislocation sites (an "interior acquisition" mechanism), where the network is locally weakened.

If the network were to acquire pentagons in its interior, then budding of the clathrin-coated membrane would involve a *dislocation-unbinding* process: a neighboring pentagon-heptagon pair would separate, causing the pentagon to move to the center of the patch and the heptagon to the edge. This scenario would be consistent with the observation that highly curved coated pits have a significantly higher proportion of isolated pentagons as compared to only slightly curved coated pits (Heuser, 1980). After a sufficient number of pentagons (namely, 12) has been produced, the bud could then somehow pinch off from the plasma membrane to form a coated vesicle. In the following, we will not speculate on the precise kinetic scenario of the pinching off, although recent immunofluorescence investigations implicate the enzyme dynamin as an agent in the fission reaction between plasma membranes and synaptic coated vesicles (Takei, 1995). Rather, we address the following question: What is the critical spontaneous curvature required for the unbinding of a dislocation trapped in an initially flat patch of clathrin-coated membrane, and is there indeed a large energy barrier for pentagon production? The unbinding of a dislocation by spontaneous curvature is viewed here as a basic, elementary process. We find that the free energy cost for creating a free pentagon indeed grows proportionally to the radius R of the disc, as noted by Kirchhausen (1993), but we find that the gain in free energy for the formation of the disclinations due to spontaneous curvature effects also is proportional to R and, at a critical threshold, is able to overcome the cost. Once unbinding is possible, there are many scenarios that can lead to the formation of coated vesicles.

Artificial membranes and tethered surfaces

Before we start our discussion of the elastic properties of the clathrin network, we will first review the existing descriptions of the budding of pure phospholipid bilayers. The budding of these simple, artificial bilayers without a clathrin network is described extensively by continuum theories that are based on the construction of an effective membrane free energy in terms of the bilayer bending curvature. Spontaneous curvature, which can be incorporated into this free energy (Helfrich, 1973), arises from the differential packing of the headgroups and the carbon backbones of the lipid molecules (Safran, 1994). Physical variables such as membrane tension and the osmotic pressure difference across the membrane give rise to various vesicle shapes such as discocytes and stomatocytes (Deuling and Helfrich, 1976), and even multiple, connected spheres (Miao et al., 1991). A generalization of the Helfrich free energy to include the bilayer nature of the membrane has been used to study red blood cell morphology more accurately (Svetina et al., 1982; Svetina and Žekš, 1983, 1989). Budding can also result from the natural bilayer asymmetry introduced by having multiple species of lipid with different packing properties (Lipowsky, 1992, 1993).

The various vesicle shapes predicted by the continuum theories have been encountered experimentally. For example, digital optical imaging of very large, one-component lecithin vesicles whose sizes are on the order of 10 μm shows shapes in the forms of discocytes, stomatocytes, and vesicles with buds (Berndl et al., 1990). Transformations between different vesicle shapes can be produced by tem-

perature changes and are attributed to an asymmetry in the thermal expansivity of the leaflets of the bilayer. Phase-contrast optical microscopy on two-component (egg phosphatidylcholine/egg phosphatidylglycerol) vesicles has shown shape transformations produced by the application of a transmembrane pH gradient (Farge and Devaux, 1992). These shape changes were found to be consistent with an asymmetrical redistribution of lipids. Thus, artificial lipid vesicle shapes have been extensively modeled and catalogued with considerable success (Lipowsky, 1992, 1993).

If we want to apply the understanding of the artificial membrane theories to the budding and vesiculation of clathrin-coated membranes, we might begin with the Helfrich theory. The Helfrich theory for the budding of clathrin-free vesicles driven by spontaneous curvature predicts that the critical spontaneous curvature required for budding is inversely proportional to the radius of the patch undergoing budding, as described in more detail below. If we gradually increase the spontaneous curvature from zero through chemical means, as suggested by Heuser's experiments, it would be energetically favorable for the larger patches to form vesicles first, rather than the smaller patches. This result is reasonable because a surface with a large area requires only a small amount of curvature to form a vesicle, whereas a surface with a small area would require much larger curvatures. Clathrin-coated vesicles, on the other hand, appear to have sizes much smaller than that of typical phospholipid bilayer vesicles. In particular, the very small clathrin cages observed by Heuser do not appear to fit the above description. It is a key point of this paper that the Helfirch theory by itself should not be applied to the vesiculation of clathrin-coated membranes.

The key missing ingredient in the above continuum theory is the clathrin network elasticity. Membrane free energies combining the Helfrich free energy with network elasticity have in fact been constructed for "tethered" surfaces. Tethered surfaces are exemplified by two-dimensional polymer networks such as polymerized Langmuir-Blodgett films or amphiphilic bilayers (see, e.g., Fendler and Tundo, 1984, and references therein) and by the spectrin-based cytoskeleton of human red blood cells (Elgsaeter et al., 1986). Tethered surfaces have also been studied theoretically for their statistical-mechanical and folding properties (Kantor, 1989). Because defects such as dislocations and disclinations can easily be accommodated, we propose that tethered surfaces are appropriate for the modeling of clathrin-coated membranes. In particular, the topological changes required by the kinetic scenarios can be addressed. We must, however, extend the existing tethered-surface model to account for an asymmetrical tethered surface due to spontaneous curvature and to allow for the spontaneous rupture of the clathrin network under a sufficient level of elastic strain.

Our model is a composite membrane representing a clathrin-coated membrane: a plasma membrane, an underlying clathrin network, and any of the assembly/adaptor proteins necessary to bind them together. In the theory of tethered surfaces, the underlying discreteness of the clathrin network enters through the inclusion two types of defects: fivefold and sevenfold disclinations. A fivefold disclination is constructed within continuum theory by removing a 60° wedge from a flat sheet and connecting the newly formed edges together, forming locally a conical structure, and a sevenfold disclination is constructed by inserting a 60° wedge into a cut in a flat sheet and connecting the edges together, forming locally a saddle-like structure. We will study the effect of the spontaneous curvature of the composite membrane on a single dislocation (i.e., a 5–7 disclination pair) embedded in the clathrin network. The continuum description of tethered surfaces containing exactly one disclination or one dislocation was given by Seung and Nelson (1988). In this paper we will generalize their theory to allow for spontaneous curvature, to study dislocation unbinding. We will show that there is a critical value of spontaneous curvature beyond which a rupturing force is generated that causes a stepwise unbinding of the dislocation. In the context of Heuser's experiments, this spontaneous curvature threshold could be thought of as a type of pH "switch" for inducing the formation of microcages. We will also discuss how this stepwise unbinding avoids the paradox posed by Kirchhausen and the result that the presence of the clathrin network allows only the smallest of coated vesicles to form.

THEORY AND MODELING

Elastic free energy of tethered surfaces: no defects

Tethered surfaces consist of a network of sites connected by flexible elastic links. If we want to model a clathrin network as a tethered surface, then the network is triangular, with every site connected to three neighboring sites. The elastic free energy of such a surface can be described in terms of two sets of variables: the principal radii of curvature at every point of the surface and the strain tensor of the network of points (Kantor, 1989). The total free energy F_t is the sum of three terms: 1) F_b, the Helfrich bending free energy describing the cost of deforming the surface; 2) F_s, the elastic energy describing the cost of straining the internal network (assuming the plasma membrane to be fluid); and 3) F_L, a line energy representing the energy decrease in joining together the edges of a patch of clathrin-coated membrane to form a coated vesicle. The bending free energy F_b is the integral over the entire surface:

$$F_b = \int d\mathbf{r}\left(\frac{1}{2}\kappa[H(\mathbf{r}) - c_0]^2 + \kappa_G K(\mathbf{r})\right). \qquad (1)$$

The first term represents the energy cost of locally deforming the surface from its preferred curvature c_0, where $H(\mathbf{r})$ is the local total curvature (given by the ratio of the sum of the principal radii of curvature divided by their product). The second term describes the energy cost of saddle-like deformations, where $K(\mathbf{r})$ is the local Gaussian curvature (given by the ratio of one divided by the product of the

principal radii of curvature). The quantities H and K are coordinate-independent, geometrical invariants characterizing the surface curvature. The contribution to c_0 by the clathrin network is controlled by the intrinsic pucker of the clathrin molecules (Kirchhausen et al., 1986). The intrinsic pucker is assumed to be dependent on chemical environmental conditions such as the pH level, the concentration of potassium and calcium ions, and the presence of membrane-associated signaling proteins. The coefficients κ and κ_G are the bending modulus and saddle-splay modulus of the surface, respectively. The bending stiffness of a clathrin-covered membrane is due to the combined effects of the bending stiffnesses of the clathrin network and that of the lipid bilayer. Bending energies of clathrin-coated membranes have not been measured, but the known bending energy of pure phospholipid bilayers (typically between 10 and $100k_BT$ or $\sim$6–60 kcal/mol) must form a lower bound. Given the ability of clathrin to form a wide range of structures, including pentagons, hexagons, heptagons, cages, cubes (Sorger et al., 1986), and tetrahedra (Heuser et al., 1987), we would expect clathrin-coated membranes to have a bending energy not much exceeding this lower bound.

The second contribution of the free energy is the elastic energy F_s due to strain in the clathrin network:

$$F_s = \frac{1}{2}\int d\mathbf{r}(2\mu u_{ij}^2 + \lambda u_{kk}^2), \tag{2}$$

where the integral is again over the entire surface. The quantities λ and μ are the Lamé coefficients, where μ is the two-dimensional shear modulus of the network and $\lambda + \mu$ is the two-dimensional compressional modulus of the network. The elastic moduli depend only on the clathrin network and have not yet been measured. Typically, two-dimensional elastic moduli are on the order of the molecular binding energy per site divided by the area per site. In our case they would be on the order of $20–30k_BT/(100\ \text{Å})^2$. We will assume below that the network can be sheared, but strongly resists extension. The quantity u_{ij} in Eq. 2 is the strain tensor:

$$u_{ij} = \frac{1}{2}(\partial_i u_j + \partial_j u_i + \partial_i u_k \partial_j u_k + \partial_i f \partial_j f), \tag{3}$$

where the vector $\mathbf{u}(\mathbf{r})$ is the in-plane displacement, and the scalar function $f(\mathbf{r})$ is the out-of-plane displacement (see Fig. 5).

The final contribution of the free energy is a line energy F_L. Upon transforming a coated pit of area πR^2 into a coated vesicle of radius $R/2$, the unsatisfied clathrin bonds at the edge of the pit are linked together with a free energy

$$F_L = 2\pi R\tau, \tag{4}$$

where the parameter τ plays the role of a line tension (free energy per unit length).

We will use this total free energy F_t to examine the fate of an initially flat network as we increase the spontaneous curvature from zero. We will first consider the case of a patch of surface with no in-plane elasticity, i.e., with $\mu = \lambda = 0$. The transformation of the patch from an open, flat state to a vesicular shape is considered to be allowed energetically if the free energy of the final state is lower than the free energy of the initial state, i.e., $F_t(\text{vesicle}) - F_t(\text{patch}) < 0$. Using Eqs. 1 and 4, it is straightforward to demonstrate that a circular patch of radius R will transform into a spherical vesicle of the same area, provided the spontaneous curvature exceeds a critical value $c_0^*(R)$, given by

$$c_0^*(R) = \frac{1}{R}\left(1 + \frac{2\kappa_G}{\kappa}\right) - \frac{\tau}{\kappa}. \tag{5}$$

It follows from Eq. 5 that vesiculation starts when the spontaneous curvature exceeds a threshold of order $1/R$: the larger the patch, the easier it vesiculates. This is the reason why, within the Helfrich theory, formation of large vesicles is expected to occur first. It should be noted, though, that for bilayer membranes consisting of mixtures of phospholipids, size selection is a more complex issue (Lipowsky, 1992, 1993). To discuss the case of nonzero elastic moduli, we first must address the question of topological defects in tethered surfaces.

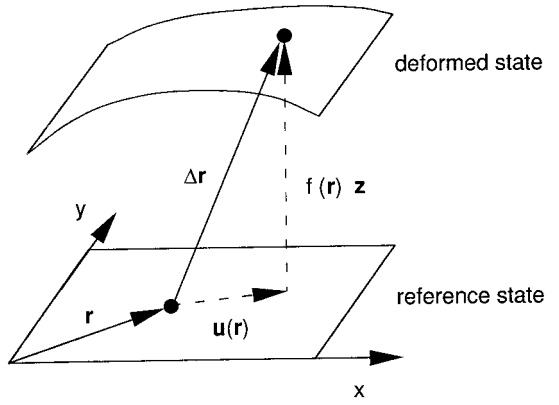

FIGURE 5 The deformation modes of a surface. The in-plane mode is described by a position-dependent vector **u**, and the function f describes the out-of-plane mode.

Topological defects

A defect in a tethered surface may be a dislocation, characterized by its Burgers vector **b**, or a disclination, characterized by its disclinicity s. The vector **b** is a lattice vector that increments the displacement vector **u** after one passage around any closed contour enclosing the dislocation line. The disclinicity s of a defect is the angle of a wedge of material that must be removed or inserted into the surface to create the defect. The underlying, discrete nature of the clathrin lattice within the patch of coated membrane imposes the possible choices for **b** and s. A fivefold disclination is produced if a 60° wedge is excised from a hexagonal

network, and the newly created edges are joined, whereas a sevenfold disclination is produced by inserting such a wedge into a hexagonal network. In Fig. 6 we show the shape of two patches of tethered surface containing either a fivefold disclination or a sevenfold disclination. The introduction of a pentagon or heptagon results in a conical or saddle-like surface, respectively.

The equations of elasticity governing the strain tensor and the curvature of tethered surfaces are discussed in the Appendix. For isolated five- and sevenfold disclinations, approximate solutions are available (see Seung and Nelson, 1988). We are interested in the unbinding of dislocations, but unfortunately, no solutions are available for dislocations. However, Seung and Nelson discuss the form of the free energy of a single dislocation for the case of zero spontaneous curvature. To include the effect of spontaneous curvature, we propose a heuristic method for finding an approximate solution for the case of the dislocation by making use of the fact that inextensible surfaces can be studied using materials such as paper or overhead transparencies, which are free to bend but are virtually impossible to stretch.

Variational construction

We constructed out of thin, flexible overhead transparencies a series of models, each containing a single dislocation. As shown in Fig. 7, dislocations can be made by a simple procedure in which first a wedge of angle s is removed from an initially flat disc of radius R and joining the cut edges together. The cone is then cut upward along a slant height to a distance corresponding to the desired b/R value. The previously removed wedge of angle s is reinserted and the edges joined together. In practice, it was difficult to construct models with $b/R < 0.1$ or $b/R > 0.8$. These models

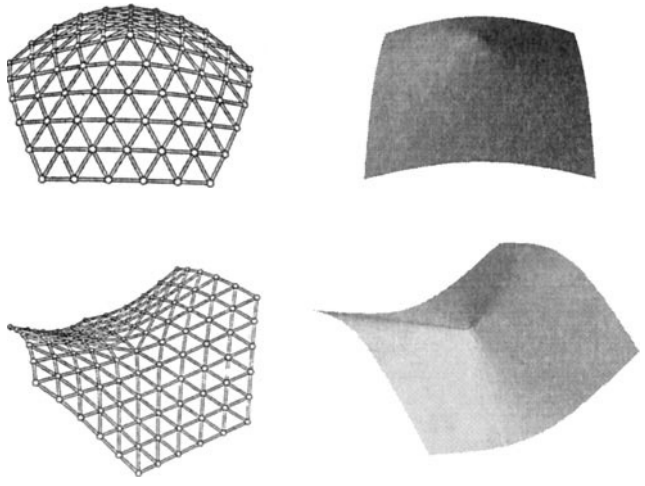

FIGURE 6 Equilibrated triangulated lattices of a fivefold disclination (*top*) and a sevenfold disclination (*bottom*), from Seung and Nelson. Also seen here are the corresponding continuum surfaces that satisfy the equilibrium equations of elasticity that account for the presence of topological defects.

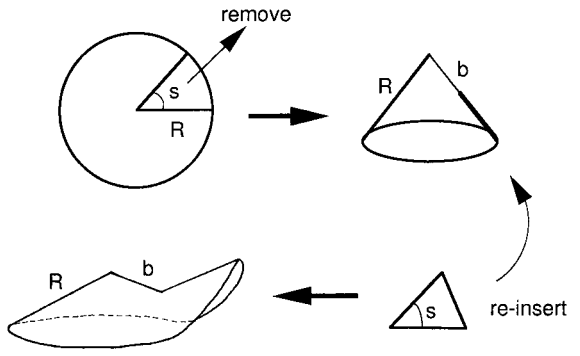

FIGURE 7 Schematic for the construction of single-dislocation surfaces. A wedge of material of angle s is removed from a disc of material, and the edges are joined. The wedge is inserted into the conical surface at a distance b from the cone vertex.

can be considered to be solutions of the equilibrium equations for inextensible surfaces with topological defects. We then use a modified superposition approach to approximate these models. To this end, we observed that these models are usually composed of four regions: a conical region, a saddle region, and an intervening nearly planar section on either side of the mirror plane. These regions are approximately delimited by two angles θ'_5 and θ'_7 (with $\theta'_5 \geq \theta'_7$), as measured from the positive x' axis (see Fig. 8). Primes are used to denote measurements with respect to the saddle vertex. The angles can be estimated by seating the conelike portion of the dislocation on a pure cone, matching the vertices without distorting either of the flexible surfaces,

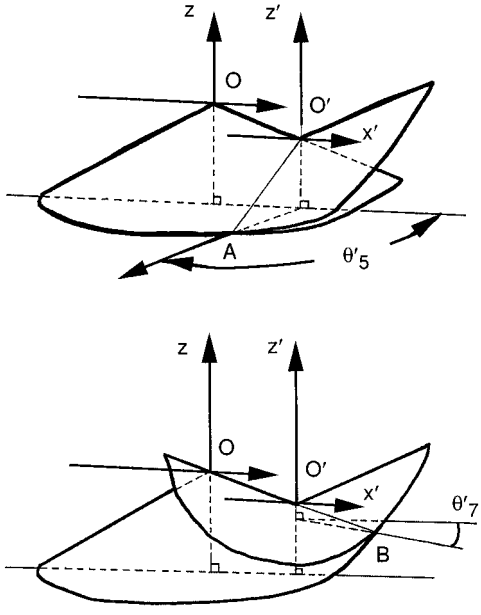

FIGURE 8 Comparison used to approximate a solution to the dislocation surface. The back halves of the surfaces are omitted for clarity. (*Top*) Comparison between a dislocation and a cone. The surfaces appear to coincide for angles between θ'_5 and $360 - \theta'_5$ degrees. (*Bottom*) Similar comparison for a dislocation and saddle with the coincident region extending from $-\theta'_7$ to θ'_7 degrees.

and recording the interval over which the two surfaces coincide. A similar fitting can be performed for the saddle-like portion of the surface. The resulting pairs of angles, for $s = 6°$, are given in Fig. 9. When b/R is less than roughly 0.5, different values for θ_5' and θ_7' are obtained, and the models show two rather flat wedges of up to ~40° each. For b/R of ~0.5 and greater, the values of the angles are nearly equal and are ~90°, and the flattened regions bounded by θ_5' and θ_7' vanish. These results indicate a type of singularity occurring near $b/R \approx 0.5$ that seems geometrical in nature. We can now study dislocation unbinding by treating the parameter b/R as a variational parameter and using the values for θ_5' and θ_7' obtained from Fig. 9. A more basic approach would be to treat all of the variables θ_5', θ_7', and b/R as variational parameters to find θ_5' and θ_7' without having to rely on the construction of models and Fig. 9. In fact, we carried out this procedure and present the mathematical details in the Appendix, where we recover the essential features of Fig. 9.

Variational free energy

We will now use the model solutions obtained in the previous section to construct a variational free energy using Eqs. 1–3. The variational free energy F_{var} will be expressed as a function of the parameter b/R, the dimensionless spacing between the disclinations. If the free energy minimum of $F_{var}(b/R)$ is at $b/R = 0$, then the patch is stable against dislocation unbinding. If the minimum is at $b/R = 1$, then the patch is stable in the unbound state. The free energy is the sum of two terms:

$$F_{var}(b/R) = F_{c_0=0}(b/R) + F_{sc}(b/R). \tag{6}$$

The first term is the dislocation free energy for zero spontaneous curvature, for which we will use the expression proposed by Seung and Nelson. The second term is the contribution due to spontaneous curvature. From Eq. 1 it follows that

$$F_{sc}(b/R) = -\kappa c_0 \int d\mathbf{r}\ \ H(\mathbf{r}) + \frac{\pi}{2}\kappa(c_0R)^2. \tag{7}$$

Note that the spontaneous curvature free energy vanishes, as it should, when $c_0 = 0$. For small deflections f (i.e., $|\tilde{\nabla}f| \ll 1$), or equivalently, small disclinicities s, the total curvature $H \approx \nabla^2 f$. The first term in Eq. 7 transforms into a boundary integral around the edge of the projection of the disc:

$$F_{sc}(b/R) \approx 2\kappa c_0 R\Lambda(b/R) + \frac{\pi}{2}\kappa(c_0R)^2, \tag{8}$$

where the function $\Lambda(b/R)$ is defined as

$$\Lambda(b/R) \equiv \frac{1}{2}\int_0^{2\pi} d\theta(\mathbf{n}\cdot\tilde{\nabla}f)|_{r=R}, \tag{9}$$

where $\mathbf{n}$ is the unit normal to the surface. The limiting values of the function $\Lambda(b/R)$ are obtained straightforwardly: for $b/R = 0$, the patch is flat, so $\Lambda(0) = 0$; for $b/R = 1$, the surface is a pure fivefold disclination for which the solution is known. It is easy to show that $\Lambda(1) \approx -\pi(s/\pi)^{1/2}$. To obtain $\Lambda(b/R)$ for intermediate values of b/R, we used the model solutions of the previous section. The method is described in the Appendix.

The free energy $F_{c_0=0}(b/R)$ of a dislocation with zero spontaneous curvature is

$$F_{c_0=0}(b/R) = K_0R^2\left(\frac{b}{R}\right)^2\left[\frac{1}{8\pi}\log(R_b/r_0) + c(\kappa_G/\kappa)\right], \tag{10}$$

as proposed by Seung and Nelson. Here the dimensionless function $c(\kappa_G/\kappa)$ depends only on the ratio of bending constants, and r_0 is the lattice spacing of the clathrin lattice. The constant $K_0 = 4\mu(\mu + \lambda)/(2\mu + \lambda)$ in Eq. 10 is the two-dimensional Young's modulus. The length scale R_b, on the order $(\kappa/K_0)^{1/2}$, is called the buckling radius. It is the radius of the area at the center of a disclination where the stresses are large enough for significant deformation of the bond network to occur.

Combining the zero and nonzero spontaneous curvature free energies in Eqs. 8 and 10, we can finally write the variational energy F_{var} for a fixed patch size R as

$$F_{var}(b/R) = K_0R^2\left(\frac{b}{R}\right)^2\left[\frac{1}{8\pi}\log\left(\frac{R_b}{r_0}\right) + c\left(\frac{\kappa_G}{\kappa}\right)\right] - 2\kappa c_0 R|\Lambda(b/R)| + \frac{\pi}{2}\kappa(c_0R)^2, \tag{11}$$

where we have explicitly taken into account the sign of Λ. The first term of Eq. 11 represents a harmonic restoring force opposing dislocation unbinding, and the second (negative) term favors dislocation unbinding due to spontaneous curvature. The last term is independent of b/R and does not contribute to the mechanical unbinding force.

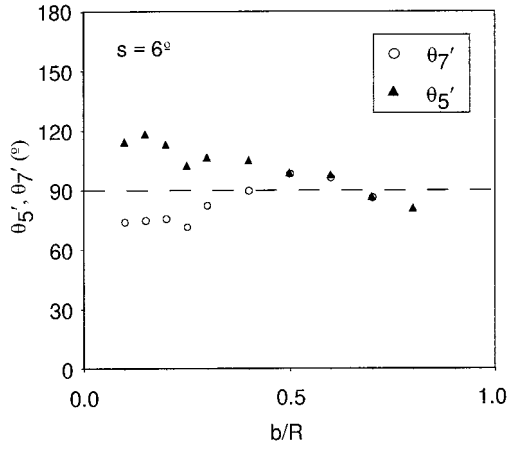

FIGURE 9 Observed overlap angles (see Fig. 8) in the hand-constructed dislocations, as a function of b/R, for disclinities of $s = \pm 6°$. The angles appear to coincide for intermediate b/R and larger.

We will discuss dislocation unbinding on the basis of Eq. 11 in the next section, but we first must point out some of the limitations of our variational free energy. Equation 11 applies to tethered surfaces that are only mildly deformed. This assumption, which was used to arrive at Eqs. 8 and 9, is valid if the disclinicity s is small compared to $(360/2\pi)°$. In fact, for clathrin networks $s = 60°$, which is not small in comparison. We do not expect, however, qualitatively new results for larger s values. A second—and more serious—limitation of Eq. 11 is the fact that we did not explicitly include the fracture of the clathrin arms in our calculation. As mentioned earlier, an energy barrier on the order of 20–30 k_BT must be overcome to break the bonds among the clathrin arms before the disclination pair can increase its spacing b. We show below that the requisite energy is implicitly provided by a mechanical force generated by an increase in the spontaneous curvature of the composite membrane.

RESULTS AND DISCUSSION

Stability condition

In this section we return to the question raised in the Introduction: What is the critical value of the spontaneous curvature c_0^* of the patch of clathrin-coated membrane composite required for dislocation unbinding? Recall that dislocation unbinding is viewed as a mechanical prerequisite of the budding process. To answer this question, there are two criteria that must be satisfied: 1) the free energy of the composite F_{var} must be lowered upon unbinding, and 2) there must be a mechanical force $-dF_{var}/db$ capable of breaking one clathrin bond. We first write the variational free energy (Eq. 11) in dimensionless form:

$$\tilde{F}_{var}(b/R) = \left(\frac{b}{R}\right)^2 - \Gamma|\Lambda(b/R)|, \tag{12}$$

where

$$\tilde{F}_{var}(b/R) \equiv \frac{F_{var}(b/R)}{K_0R^2\log(R_b/r_0)/8\pi}, \tag{13}$$

and where

$$\Gamma \equiv \frac{2\kappa c_0}{K_0R\log(R_b/r_0)/8\pi}. \tag{14}$$

(Our discussion is not affected by dropping terms independent of b/R.) The quantity Γ is a b-independent, dimensionless control parameter, proportional to the spontaneous curvature.

In Fig. 10 we show a plot of the numerically computed function $\tilde{F}_{var}(b/R)$ for a disclinicity $s = 6°$ and for various values of the dimensionless parameter Γ. We could not obtain reliable values for $\tilde{F}_{var}(b/R)$ for b/R near zero and near one, although obviously $\tilde{F}_{var}(0) = 0$ in Eq. 12. It is clear from Fig. 10 that with increasing values of the Γ parameter, the free energy minimum shifts from $b/R = 0$ to a b/R value close to one. The result of the calculations is thus surprisingly simple: dislocation unbinding is energetically allowed when the dimensionless control parameter Γ, proportional to the spontaneous curvature c_0, exceeds a critical value of order one. The unbinding allows the saddle-like disclination to move to the edge of the system, leaving behind the fivefold disclination in the center.

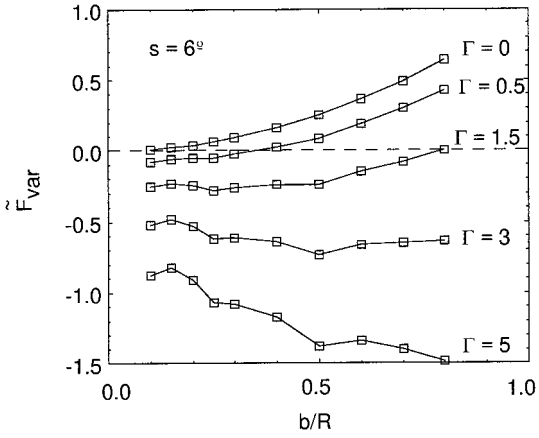

FIGURE 10 Values of dimensionless free energy versus b/R for several values of Γ for our dislocation model, using the angles in Fig. 9.

Let the critical value of the Γ parameter for dislocation unbinding be Γ^*. We can use Eq. 14 to find the corresponding critical spontaneous curvature $c_0^*(R)$ for dislocation unbinding:

$$c_0^*(R) = \frac{K_0R}{\kappa}\frac{\Gamma^*}{16\pi}\log\left(\frac{R_b}{r_0}\right). \tag{15}$$

Equation 15 is our key result. The critical spontaneous curvature for dislocation unbinding is predicted to be proportional to the radius R of the patch. The larger the patch radius, the greater the spontaneous curvature apparently needs to be to induce vesiculation. This claim is in strong disagreement with the predictions of Helfrich theory (Eq. 5), according to which large patches are more susceptible to vesiculation than small patches. The explanation can be seen from Eq. 11: the destabilizing spontaneous-curvature contribution to the free energy is linear in the patch radius R, whereas the elastic energy scales as the area πR^2 of the patch. The larger the patch size, the smaller the relative contribution from spontaneous curvature, and the dislocation in the patch has a lessened tendency to undergo unbinding.

Kirchhausen paradox revisited

We mentioned in the introductory section that, at first sight, the energy barrier against formation of free fivefold, pentagonal disclinations appears to be on the order of the bond-breaking energy E_B times $2R/r_0$, where r_0 is the lattice constant (Kirchhausen, 1993). This energy barrier is not encountered in the present theory. Fig. 10 suggests the

formation of the pentagon proceeds via a zipper-like sequence of bond fractures as the dislocation unbinds. Each of these individual steps involves an energy barrier only on the order of E_B. Another way of viewing this is by noting that the term in the free energy responsible for the dislocation unbinding is the first term of Eq. 8, which is on the order of $-\kappa c_0 R$. This term is proportional to the patch radius R. If the spontaneous curvature is large enough, it can provide the required force for the tearing of the clathrin bonds. The condition for this tearing to take place is that $-dF_{var}/db$ exceeds E_B/r_0. This condition is satisfied provided the spontaneous curvature exceeds the threshold

$$c_0^*(R) = \frac{K_0 R}{\kappa} + \frac{E_B}{\kappa r_0}. \quad (16)$$

For patch radii large compared to the lattice constant, we recover our earlier criterion, Eq. 15. We can conclude that spontaneous curvature-driven dislocation unbinding as a source of pentagon production does not involve unreasonably large energy barriers.

The critical curvature threshold given by Eq. 16 does not extend to arbitrarily large R. The free energy gain for the puckering of an individual clathrin molecule is on the order of $\kappa(c_0 r_0)^2$. If this is large compared to the fracture energy E_B of clathrin molecules, then the curvature energy is strong enough to decompose the network. The threshold curvature for this form of local fracture is

$$c_0 = \left(\frac{1}{r_0^2}\frac{E_B}{\kappa}\right)^{1/2}. \quad (17)$$

We should only use Eq. 15 for the critical curvature as long as it is less than the bound given by Eq. 17.

Vesiculation and size selection scenario

Our theory has provided us with two conditions for vesiculation in terms of the spontaneous curvature. The conventional result, Eq. 5, was obtained by comparing the free energies of a flat patch of membrane with that of a sphere. It demands that the spontaneous curvature c_0 must exceed a critical value on the order of $1/R$, where R is the patch size. We argued that Eq. 5 was derived for a fluid bilayer and that it need not be valid for a surface covered with a network. If, however, we perform a similar calculation comparing the free energies of a flat patch of tethered surface with that of a spherical surface covered by a network—including the elastic energy of the 12 pentagons—then we still find that c_0 must be at least on the order of $1/R$ for vesiculation to take place. In other words, the Helfrich criterion must still be obeyed. On the other hand, the condition Eq. 15 (or Eq. 16) for the production of free pentagons imposes a very different critical curvature, namely, a curvature proportional to R. This second criterion was not based on a comparison of free energies, but rather on finding a topological "path" allowing the production of pentagons. Membrane patches that obey the Helfrich condition (Eq. 5) but not Eq. 15 should be considered metastable. Rapid vesiculation is possible only if both conditions are satisfied. The energetics of coated-vesicle formation and the mechanics of network rupture can be simultaneously satisfied by all points in the common region, region II in Fig. 11, where $R_B < R < R_D$. These two conditions together predict the existence of a minimal value of spontaneous curvature, $c_{0,min}$, for which clathrin-coated vesicles may form. By equating Eqs. 5 and 15, we find that R_C is on the order of $(\kappa/K_0)^{1/2}$, which is curiously on the order of the buckling radius R_b (see Appendix). Using $10-100 k_B T$ as the expected, the typical order of magnitude of the bending stiffness of a bilayer plus a clathrin network, along with the typical value of clathrin bond energy, R_C, is estimated to be on the order of the lattice constant r_0 of the network. We conclude that the minimum critical spontaneous curvature $c_{0,min}^*$ is on the order of $1/R_{min}$. This result is consistent with the spontaneous curvature required to bend a single clathrin molecule up from the network and break the bond (see Eq. 17). Because continuum theories such as the tethered-surface description we have used in this paper are not expected to be valid on length scales smaller than the lattice spacing, we should not expect our theory to be quantitatively accurate if the buckling radius, on the order of $(\kappa/K_0)^{1/2}$, is comparable to, or smaller than, the lattice size.

Size distributions and experiments

Electron microscopy of coats reassembled from pure clathrin shows a rather broad distribution of coat diameters (70–125 nm), and those reassembled from clathrin in the presence of assembly/adaptor proteins show a narrow distribution around 78 nm (Zaremba and Keen, 1983). In vitro experiments involving glass-adhered plasma membranes are

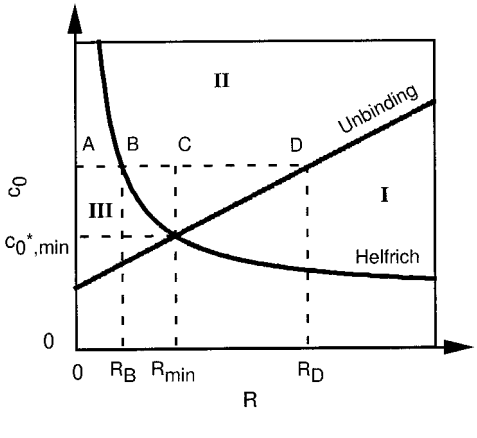

FIGURE 11 Vesiculation diagram for the theory of artificial membranes and the dislocation-unbinding model in this paper. Plotted is spontaneous curvature versus radius of composite patch size. Defect-free membranes are energetically allowed to vesiculate in regions I and II, whereas dislocation unbinding is permitted in clathrin networks in regions II and III. The common region II denotes favorable budding and vesiculation of coated pits. Because R_{min} is estimated to be on the order of the clathrin lattice spacing, only patches with radii ranging from R_{min} to R_D may form coated vesicles.

known to support clathrin reassembly as well as growth (Lin et al., 1991), and to lead to the formation of so-called microcages devoid of plasma membrane (Heuser, 1989).

We interpret our results in the following way. Assume a preexisting patch of radius R_D larger than R_C, the buckling radius, with a spontaneous curvature of zero (see Fig. 11). As the spontaneous curvature c_0 is increased beyond the minimum value $c^*_{0,\min}$ by the adjustment of chemical parameters such as pH, pentagon production becomes possible, but only for patches with a size on the order of the buckling radius. Our patch remains stable. Once c_0 becomes equal to $c^*_0(R_D)$, as given by Eq. 15, pentagon production is possible and vesiculation can take place. It follows that if we have a distribution of patch sizes, then the first vesicles to form are expected to have a size on the order of the buckling radius, $(\kappa/K_0)^{1/2}$. In general, vesiculation should be possible only if the spontaneous curvature exceeds the threshold value $c^*_{0,\min} = (K_0/\kappa)^{1/2}$.

Alternatively, suppose we "set" the pH level and grow clathrin patches on a membrane with increasing R. If the spontaneous curvature is less than the threshold $c^*_{0,\min}$, then vesiculation should never take place. If the spontaneous curvature exceeds this threshold, vesiculation may take place as soon as R exceeds $R_{\min}$ in region II in Fig. 11. Because $R_{\min}$ is, according to our estimates, not much larger than the size of a clathrin molecule, we must expect, in this scenario, formation of the smallest coated vesicles possible. Our theory thus predicts the presence of a clear pH threshold for the formation of coated vesicles, namely when c_0 equals $c^*_{0,\min}$, and a vesicle size distribution that is peaked at the smallest permitted coated vesicle sizes. Our argument would be inconsistent with distributions favoring large coated vesicles in these types of in vitro experiments.

CONCLUSION

We have presented a physical study of clathrin-coated membranes, using a composite plasma membrane/clathrin lattice model that accounts for the clathrin network topology in a natural way and possess an intrinsic, spontaneous curvature, as motivated by acidification experiments of clathrin lattices. We have discussed vesiculation and size selection of coated vesicles, finding that the spontaneous vesiculation of large regions of clathrin-coated membrane having a modest spontaneous curvature is disallowed, because of the presence of the clathrin network. The nature of this limitation is the mechanical constraint of breaking clathrin bonds in the lattice to introduce the pentagons necessary to form the clathrin coat. For spontaneous curvatures larger than a critical value, this limitation is overcome, leading only to the smallest possible coated vesicles. Finally, our theory cannot prove that vesiculation must take place. For that, one would have to go beyond the present theory and develop a microscopic model of clathrin and the clathrin network.

APPENDIX

We describe here the various mathematical details omitted above. We will summarize the theory of tethered surfaces containing arbitrary dislocations and disclinations in the absence of spontaneous curvature (Seung and Nelson, 1988), and discuss a mathematical treatment of the dislocation surface suggested by our constructed models.

Equilibrium for tethered surfaces with and without topological defects

Equations of equilibrium result from the minimization of the total free energy of the tethered surface with respect to all possible deformations, described by the in-place displacement vector $\mathbf{u}(\mathbf{r})$ and the out-of-plane deformation $f(\mathbf{r})$ (see Fig. 5). Assuming small variations in $\mathbf{u}$ and f (i.e., $|\nabla u_i| \ll 1$ and $|\nabla f| \ll 1$), one equilibrium condition is

$$\kappa\nabla^4 f = \frac{\partial^2\chi}{\partial y^2}\frac{\partial^2 f}{\partial x^2} + \frac{\partial^2\chi}{\partial \chi^2}\frac{\partial^2 f}{\partial y^2} - 2\frac{\partial^2\chi}{\partial x\partial y}\frac{\partial^2 f}{\partial x\partial y}, \qquad \text{(A1)}$$

where the surface bending energy is κ. The auxiliary function $\chi(\mathbf{r})$ is called the *Airy stress function*, defined through the relation $\sigma_{ij}(\mathbf{r}) = \epsilon_{ik}\epsilon_{jl}\partial_k\partial_l\chi(\mathbf{r})$, in which the stress tensor σ_{ij}, a function of the strain tensor, is expressed as $\sigma_{ij} = 2\mu u_{ij} + \lambda u_{kk}\delta_{ij}$. The Airy function, found from the condition

$$\nabla^4\chi(\mathbf{r}) = -K_0 K(\mathbf{r}), \qquad \text{(A2)}$$

is the second equilibrium condition. The variable $K_0 = 4\mu(\mu + \lambda)/(2\mu + \lambda)$ is the two-dimensional Young's modulus, and $K(\mathbf{r})$ is the Gaussian curvature. Physically, K_0 is a proportionality constant relating in-plane stress build-up due to in-plane stretching. Equations A1 and A2 are the von Kármán equations of equilibrium; this is a set of coupled, nonlinear partial differential equations that can be solved in only a number of special cases. Defects such as disclinations and dislocations can be accounted for in this formalism (Seung and Nelson, 1988). If s_α is the disclinicity of the αth defect, located at a position $\mathbf{r}_\alpha$, and b_i^β is the ith component of the Burgers vector of a dislocation at $\mathbf{r}_\beta$, then the resulting equations of equilibrium in the absence of spontaneous curvature are

$$\kappa\nabla^4 f = \frac{\partial^2\chi}{\partial y^2}\frac{\partial^2 f}{\partial x^2} + \frac{\partial^2\chi}{\partial x^2}\frac{\partial^2 f}{\partial y^2} - 2\frac{\partial^2\chi}{\partial x\partial y}\frac{\partial^2 f}{\partial x\partial y} \qquad \text{(A3)}$$

$$s(\mathbf{r}) - K(\mathbf{r}) = \frac{1}{K_0}\nabla^4\chi = -\frac{\partial^2 f}{\partial x^2}\frac{\partial^2 f}{\partial y^2} + \left(\frac{\partial^2 f}{\partial x\partial y}\right)^2 + \sum_\alpha s_\alpha\delta(\mathbf{r} - \mathbf{r}_\alpha) - \sum_\beta b_i^\beta\epsilon_{ik}\partial_k\delta(\mathbf{r} - \mathbf{r}_\beta). \qquad \text{(A4)}$$

The new quantity appearing in Eq. A4 is $s(\mathbf{r})$, the disclination source density. Physically, the Gaussian curvature $K(\mathbf{r})$ in Eq. A4 screens out stress arising from the presence of the topological defects in the tethered membrane. These equations admit solutions only in the limit of an unstretchable or inextensible surface, whose elastic constants μ and λ are effectively infinite. This regime corresponds to either 1) taking the formal limit $K_0 \to \infty$ while the stress function $\chi(\mathbf{r})$ remains finite, or 2) having that $r_0^2 K_0/\kappa$ is large compared to unity, where r_0 is the lattice constant of the underlying lattice. For a conical disclination ($s > 0$) at the origin, the solution of Eqs. A3 and A4 is

$$\chi = \kappa\log(r/r_0) \qquad \text{(A5)}$$

$$f = \alpha r, \qquad \text{(A6)}$$

with $\alpha = [1/(1 - s/2\pi)^2 - 1]^{1/2} \approx (s/\pi)^{1/2}$ for small s. The constant r_0 is the lattice spacing, and $r^2 = x^2 + y^2$ is the square of the in-plane distance.

For an isolated, saddle-like disclination ($s < 0$) at the origin, the solutions are

$$\chi = -3\kappa \log(r/r_0) \tag{A7}$$

$$f = \begin{cases} -\beta r \cos(2\theta), \text{ or} \\ -\beta r \sin(2\theta) \end{cases} \tag{A8}$$

with $\theta = \tan^{-1}(y/x)$, and, for small s, $\beta \approx (2|s|/3\pi)^{1/2}$.

By a using a combination of analytic and scaling arguments, Seung and Nelson examined the free energy of a single dislocation in a flat surface and in a buckled surface. For the buckled states, they found that a single dislocation consisted of two concentric regions—a flat section and a buckled section—separated by a length scale called the buckling radius, R_b, where the inner (outer) region is energetically stable when flat (buckled). The resulting free energy for an inextentional surface (in the absence of spontaneous curvature) is largely due to the free energy of the flat region, and is given approximately by

$$\frac{1}{K_0 b^2} F(c_0 = 0) \approx \frac{1}{8\pi} \log\left(\frac{R_b}{r_0}\right) + c\left(\frac{\kappa_G}{\kappa}\right). \tag{A9}$$

The dimensionless function $c(\kappa_G/\kappa)$ accounts for the free energy contribution outside the radius of buckling and is independent of b. In our dislocation unbinding scenario, R_b is on the order of $(\kappa/K_0)^{1/2}$.

Variational mathematical model

We examined a mathematical representation of a single dislocation as motivated by the hand-constructed models discussed in the main text above, and the results are in general agreement with the stability diagram and vesiculation criteria discussed above, with a few additional artifacts. Let θ' be an angle as measured from the positive x' axis in the $x'y'$ plane, where primes denote coordinates relative to the saddle vertex (see Fig. 8). The dislocation surface is then approximated by the function

$$f(\mathbf{r}) = \begin{cases} f_7(\mathbf{r}), & \text{if } 0 \le \theta' \le \theta_7' \\ f_{pl}(\mathbf{r}), & \text{if } \theta_7' \le \theta' \le \theta_5' \\ f_5(\mathbf{r}), & \text{if } \theta_5' \le \theta' \le \pi, \end{cases} \tag{A10}$$

with the restriction that $\theta_7' \le \theta_5'$. Note that the $x'z'$ and xz planes are planes of symmetry. If the vertex of the conical section is placed at the origin, the function f_5 is given by Eq. A6, and we use the cosine form of Eq. A8 for f_7 in the form

$$f_7(x,y) = \frac{b\alpha}{\sqrt{1+\alpha^2}} - \beta\left[\left(x - \frac{b}{\sqrt{1+\alpha^2}}\right)^2 + y^2\right]^{1/2} \times \cos\left[2\tan^{-1}\left(\frac{y}{x - b/\sqrt{1+\alpha^2}}\right)\right], \tag{A11}$$

with $\alpha \approx (s/\pi)^{1/2}$ and $\beta \approx (2|s|/3\pi)^{1/2}$. For s much smaller than 60°, this form of f_7 corresponds to placing the vertex of a pure-saddle surface a distance b down along the slant height of the cone in the x direction. The region given by $f_{pl}(\mathbf{r})$ is a plane determined by two vectors originating from the saddle vertex and extending toward the points where the half-planes delimited by θ_5' and θ_7' intersect the edge of the surface. The function $f(\mathbf{r})$ is now a single surface that approximates a single dislocation surface. There is, in general, a small jump discontinuity between the cone and plane surfaces at $\theta' = \theta_5'$, and an angular discontinuity between the saddle and planar regions at $\theta' = \theta_7'$. These small, mathematical discontinuities are not intended to be related to the bond-breaking scenario we argue occurs in the dislocation unbinding process of clathrin-coated membranes.

Finding the optimal values of the angles θ_5' and θ_7' is more difficult than fitting surfaces together. In addition to the free energies in Eqs. 1, 2, and 4, we add a fourth term, F_{pc}, representing the "error" in matching the surfaces at θ_5' and θ_7'. F_{pc} is taken as the continuum limit of a discrete harmonic bending energy as formulated for triangulated networks. If $\mathbf{n}_\alpha(\mathbf{r})$ and $\mathbf{n}_\beta(\mathbf{r})$ are the normal unit vectors of the facets on either side of the saddle-plane or cone-plane interfaces, then the discrete bending energy is

$$F_{pc}^{discrete} = \frac{1}{2}\tilde{\kappa} \sum_{\langle\alpha,\beta\rangle} |\mathbf{n}_\alpha - \mathbf{n}_\beta|^2, \tag{A12}$$

where $\tilde{\kappa}$ is a new bending constant and the sum is taken over neighboring facets along the interface. Taking the continuum limit, we have

$$F_{pc} \equiv F_{pc}^{continuum} = \tilde{\kappa} \lim_{r_0 \to 0} \frac{\psi(\theta_5', \theta_7')}{r_0}, \tag{A13a}$$

and

$$\psi(\theta_5', \theta_7') = \frac{1}{2}\int d\ell (1 - \cos\gamma_{\alpha,\beta}), \tag{A13b}$$

where r_0 would be the effective lattice spacing a clathrin-free membrane, and $\gamma_{\alpha,\beta}$ is the angle between the unit normals $\mathbf{n}_\alpha(\mathbf{r})$ and $\mathbf{n}_\beta(\mathbf{r})$. The integral is evaluated along the four interfaces between the regions. We now must minimize the total free energy $F_t = F_b + F_s + F_L + F_{pc}$ with respect to displacements and the angles θ_5' and θ_7'. F_{pc} can be minimized independently of the other terms, and the minimizations of the functions $\psi(\theta_5', \theta_7')$ and F_{pc} with respect to θ_5' and θ_7' and are equivalent. The details of the analytical derivation of $\psi(\theta_5', \theta_7')$ are presented below. The optimal angles θ_5' and θ_7' were then determined as a function of b/R and s, using the method of steepest descents. Fig. 12 shows the optimal values of θ_5' and θ_7' that minimize ψ as a function of b/R for $s = 6°$. At large b/R, the optimal variational angles become equal, just as seen with the hand-constructed models in Fig. 9, but there is a noticeable disagreement in the values of the angles. One variational angle would appear to suffice for large b/R.

To examine the stability of the constructed surface, we show in Fig. 13 the numerically computed dimensionless variational free energy $\tilde{F}_{var}$ as a function of b/R for several values of the parameter Γ with $s = 6°$. For $\Gamma < 0.28$, the minimum of $\tilde{F}_{var}$ is at $b/R = 0$. For $0.28 < \Gamma < 3.53$, the minimum occurs at $b/R = 0.2$. Finally, for $\Gamma > 3.53$, we reach full unbinding with $b/R = 1$. Again, as in the case of our hand-constructed models, full dislocation unbinding takes place when the dimensionless parameter Γ exceeds a critical value Γ^* of order one.

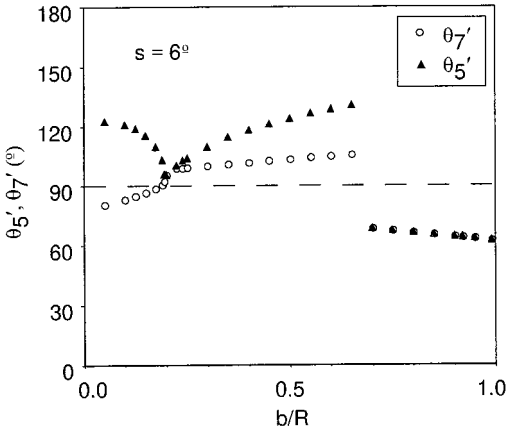

FIGURE 12 Optimal, variational overlap angles for $s = \pm 6°$ for the mathematical representation of the dislocation, as suggested by the hand-constructed models.

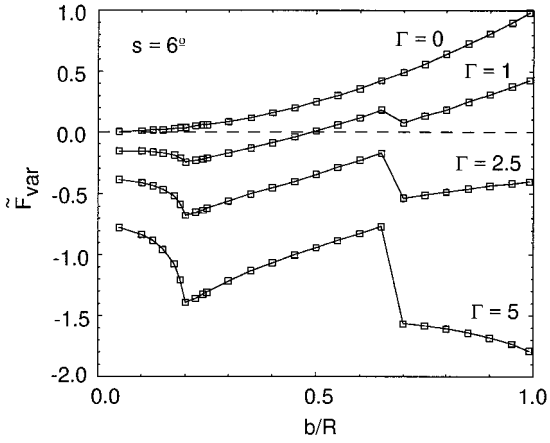

FIGURE 13 Values of dimensionless free energy versus b/R for several values of Γ for the mathematical dislocation model, using the angles in Fig. 12.

Analytic derivations

To derive the error measure $\psi(\theta_5', \theta_7')$ in Eq. A13, we define $\mathbf{n}_5$ and $\mathbf{n}_7$ to be the outward normal unit vectors to the cone and saddle surfaces, respectively. The normal unit vector $\mathbf{n}_{\rm pl} = (n_{\rm pl}^{(x)}, n_{\rm pl}^{(y)}, n_{\rm pl}^{(z)})$ to the plane $f_{\rm pl}$ is then determined from the vectors $\mathbf{O'A}$ and $\mathbf{O'B}$ as in Fig. 8. Integrating $\psi(\theta_5', \theta_7')$ along the contours, we find

$$\psi(\theta_5', \theta_7') = h_5 + h_7(1 - \mathbf{n}_7 \cdot \mathbf{n}_{\rm pl}) - \frac{1}{\sqrt{\alpha^2 + 1}}\{\alpha\tau b \times [n_{\rm pl}^{(x)} \sin\theta_5' - n_{\rm pl}^{(y)} \cos\theta_5']\sin\theta_5' + h_5 n_{\rm pl}^{(z)} + \alpha(n_{\rm pl}^{(x)} \cos\theta_5' + n_{\rm pl}^{(y)} \sin\theta_5')(X^{1/2} - b)\}, \quad \text{(A13)}$$

with

$$\tau \equiv \log\left|\frac{\sqrt{X} + h_5 + b\cos\theta_5'}{b(1 + \cos\theta_5')}\right| \quad \text{(A14)}$$

$$X \equiv b^2 + 2bh_5\cos\theta_5' + h_5^2 \quad \text{(A15)}$$

$$h_{\rm i} \approx -b\cos\theta_{\rm i}' + [1 - (b\sin\theta_{\rm i}')^2]^{1/2}, \quad i = 5, 7. \quad \text{(A16)}$$

Two disclinations of opposite s annihilate each other in the limit $b/R \to 0$, in principle, resulting in a flat surface. In the limit where both $b/R \to 0$ and $s \to 0$, we have that $\psi(\theta_5', \theta_7') \to 0$, but for nonzero s the error measure ψ is nonzero in the limit $b/R \to 0$. This result calls into question our mathematical representation of the dislocation surface when b/R is small. To estimate a lower bound on the valid range of b/R, if we take the average radius of a coated pit to be 110 nm (Heuser, 1980) and the lattice constant of 170 Å as b, we would then expect the range $0.15 < b/R \le 1$ to be valid.

Finally, the integral $\Lambda(b/R)$ in Eq. 9 can be divided into saddle, plane, and cone regions:

$$\Lambda = \int_{\varphi 5}^{\pi} {\rm d}\lambda \frac{\partial f_5}{\partial r}\bigg|_{\rm r=R} + \int_0^{\varphi 7} {\rm d}\lambda(\mathbf{n}\cdot\vec{\nabla}f_7)\bigg|_{\rm r=R} + \int_{\varphi 7}^{\varphi 5} {\rm d}\lambda(\mathbf{n}\cdot\vec{\nabla}f_{\rm pl})|_{\rm r=R}, \quad \text{(A17)}$$

where

$$\varphi_{\rm i} = \begin{cases} \sin^{-1}(h_{\rm i}\sin\theta_{\rm i}'), & \text{for } \theta_{\rm i}' \text{ in quadrant I} \\ \pi - \sin^{-1}(h_{\rm i}\sin\theta_{\rm i}'), & \text{for } \theta_{\rm i}' \text{ in quadrant II,} \end{cases}$$

$$i = 5, 7. \quad \text{(A18)}$$

Upon simplification, Eq. A18 becomes

$$\Lambda = \int_0^{\varphi 7} {\rm d}\lambda\left(\cos\lambda\frac{\partial f_7}{\partial x}\bigg|_{\rm r=R} + \sin\lambda\frac{\partial f_7}{\partial y}\bigg|_{\rm r=R}\right) + \alpha(\varphi_5 - \pi). \quad \text{(A19)}$$

We thank Dr. J. Heuser for providing us with images of clathrin networks, Dr. A. C. Steven for images of clathrin molecules, and Profs. F. Mackintosh, U. Seifert, and M. Wortis for helpful discussions. We particularly thank the referees for bringing relevant literature to our attention.

This work was supported by DMR grant no. 9407741.

REFERENCES

Alberts, B., D. Bray, J. Lewis, M. Raff, K. Roberts, and J. D. Watson. 1994. *Molecular Biology of the Cell*, 3rd Ed. Garland, New York.

Anderson, R. G. W., J. L. Goldstein, and M. S. Brown. 1976. Localization of low density lipoprotein receptors on plasma membrane of normal human fibroblasts and their absence in cells from a familial hypercholesterolemia homozygote. *Proc. Natl. Acad. Sci. USA.* 73:2434–2438.

Berndl, K., J. Käs, R. Lipowsky, E. Sackmann, and U. Seifert. 1990. Shape transformations of giant vesicles: extreme sensitivity to bilayer asymmetry. *Europhys. Lett.* 13:659–664.

Bomsel, M., C. de Paillerets, H. Weintraub, and A. Alfsen. 1986. Lipid bilayer dynamics in plasma and coated vesicle membranes from bovine adrenal cortex. Evidence of two types of coated vesicle involved in the LDL receptor traffic. *Biochim. Biophys. Acta.* 859:15–25.

Braell, W. A., D. M. Schlossman, S. L. Schmid, and J. E. Rothman. 1984. Dissociation of clathrin coats coupled to the hydrolysis of ATP: role of an uncoating ATPase. *J. Cell Biol.* 99:734–741.

Crowther, R. A., J. T. Finch, and B. M. F. Pearse. 1976. On the structure of coated vesicles. *J. Mol. Biol.* 103:785–798.

Crowther, R. A., and B. M. F. Pearse. 1981. Assembly and packing of clathrin into coats. *J. Cell Biol.* 91:790–797.

Deuling, H. J., and W. Helfrich. 1976. The curvature elasticity of fluid membranes: a catalogue of vesicle shapes. *J. Phys. (France).* 37: 1335–1345.

Elgsaeter A., B. T. Stokke, A. Mikkelsen, and D. Branton. 1986. The molecular basis of erythrocyte shape. *Science.* 234:1217–1223.

Farge, E., and P. F. Devaux, 1992. Shape changes of giant liposomes induced by an asymmetric transmembrane distribution of phospholipids. *Biophys. J.* 61:347–357.

Fendler, J. H., and P. Tundo. 1984. Polymerized surfactant aggregates: characterization and utilization. *Acc. Chem. Res.* 17:3–8.

Goldstein, J. L., R. G. W. Anderson, and M. S. Brown. 1979. Coated pits, coated vesicles, and receptor-mediated endocytosis. *Nature.* 279: 679–685.

Harrison, S. C., and T. Kirchhausen. 1983. Clathrin, cages, and coated vesicles. *Cell.* 33:650–652.

Helfrich, W. 1973. Elastic properties of lipid bilayers: theory and possible experiments. *Z. Naturforsch.* 28c:693–703.

Heuser, J. 1980. Three-dimensional visualization of coated vesicle formation in fibroblasts. *J. Cell Biol.* 84:560–583.

Heuser, J. 1989. Effects of cytoplasmic acidification on clathrin lattice morphology. *J. Cell Biol.* 108:401–411.

Heuser, J. E., J. H. Keen, L. M. Amende, R. E. Lippoldt, and K. Prasad. 1987. Deep-etch visualization of 27S clathrin: a tetrahedral tetramer. *J. Cell Biol.* 105:1999–2009.

Heuser, J., and T. Kirchhausen. 1985. Deep-etch views of clathrin assemblies. *J. Ultrastruct. Res.* 92:1–27.

Jin, A., and R. Nossal. 1993. Topological mechanisms involved in the formation of clathrin-coated vesicles. *Biophys. J.* 65:1523–1537.

Kanaseki, T., and K. Kadota. 1969. The "vesicle in a basket." *J. Cell Biol.* 42:202–220.

Kantor, Y. 1989. Properties of tethered surfaces. *In* Statistical Mechanics of Membranes and Surfaces, Vol. 5. D. Nelson, T. Piran, and S. Weinberg, eds. World Scientific, Teaneck, NJ. 115–136.

Kedersha, N. L., D. F. Hill, K. E. Kronquist, and L. H. Rome. 1986. Subpopulations of liver coated vesicles resolved by preparative agarose gel electrophoresis. *J. Cell Biol.* 103:287–297.

Kirchhausen, T. 1993. Coated pits and coated vesicles—sorting it all out. *Curr. Opin. Struct. Biol.* 3:182–188.

Kirchhausen, T., and S. C. Harrison. 1981. Protein organization in clathrin trimers. *Cell.* 23:755–761.

Kirchhausen, T., and S. C. Harrison. 1984. Structural domains of clathrin heavy chains. *J. Cell Biol.* 99:1725–1734.

Kirchhausen, T., S. C. Harrison, and J. Heuser. 1986. Configuration of clathrin trimers: evidence from electron microscopy. *J. Ultrastruct. Mol. Struct. Res.* 94:199–208.

Larkin, J. M., W. C. Donzell, and R. G. W. Anderson. 1986. Potassium-dependent assembly of coated pits: new coated pits form as planar clathrin lattices. *J. Cell Biol.* 103:2619–2627.

Lin, H. C., M. S. Moore, D. A. Sanan, and R. G. W. Anderson. 1991. Reconstitution of clathrin-coated pit budding from plasma membranes. *J. Cell Biol.* 114:881–891.

Lipowsky, R. 1992. Budding of membranes induced by intramembrane domains. *J. Phys. (France).* 2:1825–1840.

Lipowsky, R. 1993. Domain-induced budding of fluid membranes. *Biophys. J.* 64:1133–1138.

Lord, E. A., and C. B. Wilson. 1984. The Mathematical Description of Shape and Form. Halsted Press, New York.

Miao, L., B. Fourcade, M. Rao, M. Wortis, and R. K. P. Zia. 1991. Equilibrium budding and vesiculation in the curvature model of fluid lipid vesicles. *Phys. Rev. A.* 43:6843–6856.

Moore, M. S., D. T. Mahaffey, F. M. Brodsky, and R. G. W. Anderson. 1987. Assembly of clathrin-coated pits onto purified plasma membranes. *Science.* 236:558–563.

Pastan, I. H., and M. C. Willingham. 1981. Receptor-mediated endocytosis of hormones in cultured cells. *Annu. Rev. Physiol.* 43:239–250.

Pearse, B. M. F. 1975. Coated vesicles from pig brain: purification and biochemical characterization. *J. Mol. Biol.* 97:93–98.

Pearse, B. M. F. 1980. Coated vesicles. *Trends Biol. Sci.* 5:131–134.

Pearse, B. M. F. 1989. Characterization of coated vesicle adaptors: their reassembly with clathrin and with recycling receptors. *Methods Cell Biol.* 31:229–246.

Pearse, B. M. F., and M. S. Bretscher. 1981. Membrane recycling by coated vesicles. *Annu. Rev. Biochem.* 50:85–101.

Pearse, B. M. F., and R. A. Crowther. 1987. Structure and assembly of coated vesicles. *Annu. Rev. Biophys. Biophys. Chem.* 16:49–68.

Perry, M. M., and A. B. Gilbert. 1979. Yolk transport in the ovarian follicle of the hen (*Gallus domesticus*): lipoproteinlike particles at the periphery of the oocyte in the rapid growth phase. *J. Cell Sci.* 39:257–272.

Roth, T. F., and K. R. Porter. 1964. Yolk protein uptake in the oocyte of the mosquito *Aedes aegypti L. J. Cell Biol.* 20:313–332.

Safran, S. A. 1994. Flexible interfaces. *In* Statistical Thermodynamics of Surfaces, Interfaces, and Membranes. Addison-Wesley, New York. 179–212.

Seung, H. S., and D. R. Nelson. 1988. Defects in flexible membranes with crystalline order. *Phys. Rev. A.* 38:1005–1018.

Shraiman, B. I. 1997. On the role of assembly kinetics in determining the structure of clathrin cages. *Biophys. J.* 72:953–957.

Sorger, P. K., R. A. Crowther, J. T. Finch, and B. M. F. Pearse. 1986. Clathrin cubes: an extreme variant of the normal cage. *J. Cell Biol.* 103:1213–1219.

Steven, A. C., J. F. Hainfeld, J. S. Wall, and C. J. Steer. 1983. Mass distributions of coated vesicles isolated from liver and brain: analysis by scanning transmission electron microscopy. *J. Cell Biol.* 97:1714–1723.

Svetina, S., A. Ottova-Leitmannová, and R. Glaser. 1982. Membrane bending energy in relation to bilayer couples concept of red blood cell shape transformations. *J. Theor. Biol.* 94:13–23.

Svetina, S., and B. Žekš. 1983. Bilayer couple hypothesis of red cell shape transformations and osmotic hemolysis. *Biomed. Biochim. Acta.* 42: 86–90.

Svetina, S., and B. Žekš. 1989. Membrane bending energy and shape determination of phospholipid vesicles and red blood cells. *Eur. Biophys. J.* 17:101–111.

Takei, K., P. S. McPherson, S. L. Schmid, and P. De Camilli, 1995. Tubular membrane invaginations coated by dynamin rings are induced by GTP-γS in nerve terminals. *Nature.* 374:186–190.

Ungewickell, E., and D. Branton. 1981. Assembly units of clathrin coats. *Nature.* 289:420–422.

Vigers, G. P. A., R. A. Crowther, and B. M. F. Pearse. 1986. Three-dimensional structure of clathrin cages in ice. *EMBO J.* 5:529–534.

von Kármán, T. 1956. Festigkeitsprobleme im Maschinenbau. *In* Collected Works, Vol. 1. Butterworths Scientific, London.

Zaremba, S., and J. H. Keen. 1983. Assembly polypeptides from coated vesicles mediate reassembly of unique clathrin coats. *J. Cell Biol.* 97:1339–1347.